



This is a repository copy of *Semi-active inerters using magnetorheological fluid: a feasibility study*.

White Rose Research Online URL for this paper:  
<http://eprints.whiterose.ac.uk/140266/>

Version: Published Version

---

**Proceedings Paper:**

Tipuric, M., Deastra, P. [orcid.org/0000-0002-1709-4686](https://orcid.org/0000-0002-1709-4686), Wagg, D. [orcid.org/0000-0002-7266-2105](https://orcid.org/0000-0002-7266-2105) et al. (1 more author) (2018) Semi-active inerters using magnetorheological fluid: a feasibility study. In: Proceedings of SPIE. SPIE Smart Structures and Materials & Nondestructive Evaluation and Health Monitoring, 04-08 Mar 2018, Denver, Colorado. SPIE . ISBN 9781510616868

<https://doi.org/10.1117/12.2300749>

---

Copyright 2018 Society of Photo Optical Instrumentation Engineers (SPIE). One print or electronic copy may be made for personal use only. Systematic reproduction and distribution, duplication of any material in this publication for a fee or for commercial purposes, or modification of the contents of the publication are prohibited. Matthew Tipuric, Predaricka Deastra, David Wagg, Neil Sims, "Semi-active inerters using magnetorheological fluid: a feasibility study," Proc. SPIE 10595, Active and Passive Smart Structures and Integrated Systems XII, 105951H (16 March 2018); <http://doi.org/10.1117/12.2300749>

**Reuse**

Items deposited in White Rose Research Online are protected by copyright, with all rights reserved unless indicated otherwise. They may be downloaded and/or printed for private study, or other acts as permitted by national copyright laws. The publisher or other rights holders may allow further reproduction and re-use of the full text version. This is indicated by the licence information on the White Rose Research Online record for the item.

**Takedown**

If you consider content in White Rose Research Online to be in breach of UK law, please notify us by emailing [eprints@whiterose.ac.uk](mailto:eprints@whiterose.ac.uk) including the URL of the record and the reason for the withdrawal request.



[eprints@whiterose.ac.uk](mailto:eprints@whiterose.ac.uk)  
<https://eprints.whiterose.ac.uk/>

# PROCEEDINGS OF SPIE

[SPIDigitalLibrary.org/conference-proceedings-of-spie](https://SPIDigitalLibrary.org/conference-proceedings-of-spie)

## Semi-active inerters using magnetorheological fluid: a feasibility study

Matthew Tipuric, Predaricka Deastra, David Wagg, Neil Sims

Matthew Tipuric, Predaricka Deastra, David Wagg, Neil Sims, "Semi-active inerters using magnetorheological fluid: a feasibility study," Proc. SPIE 10595, Active and Passive Smart Structures and Integrated Systems XII, 105951H (16 March 2018); doi: 10.1117/12.2300749

**SPIE.**

Event: SPIE Smart Structures and Materials + Nondestructive Evaluation and Health Monitoring, 2018, Denver, Colorado, United States

# Semi-active inerters using magnetorheological fluid: a feasibility study

Matthew Tipuric<sup>a,b</sup>, Predaricka Deastra<sup>b</sup>, David Wagg<sup>b</sup>, and Neil Sims<sup>b</sup>

<sup>a</sup>Industrial Doctorate Centre in Machining Science, Advanced Manufacturing Research Centre with Boeing, University of Sheffield, Rotherham, S60 5TZ, UK

<sup>b</sup>Department of Mechanical Engineering, Sir Frederick Mappin Building, Mappin Street, Sheffield, S1 3JD, UK

## ABSTRACT

An inverter is a mechanical analogue to a capacitor, where the force across the device is proportional to relative, rather than absolute, acceleration. This concept can offer attractive performance in a wide variety of engineering vibration problems, because the engineer can tune the device without dramatically increasing the physical mass of the structure. Consequently, there have been many studies over the last two decades that have explored their application to bridge vibrations, seismic isolation of tall buildings, vehicle suspensions, and other engineering problems.

Several configurations of inverter systems have been proposed, typically involving the inverter in a vibration absorber, or by using the inverter as part of an isolation system. However, to date there have been limited studies that have explored the combination of inverters with semi-active devices such as magnetorheological fluid dampers. Furthermore, because one manifestation of inverters involves the use of hydraulic fluid, it is possible for magnetorheological effects to be integrated into the inverter itself.

The present study investigates the feasibility of this approach for practical scenarios. A quasi-static model is developed, combining an existing model of a fluid inverter with simplified models for magnetorheological fluids. The trade-off between damping performance and inverter performance is explored. The model is then used in a case study, where its potential use in a control strategy known as a parallel-layout inverter damper is investigated.

**Keywords:** helical inverter, magnetorheological fluid, semi-active, parallel viscous inverter damper

## 1. INTRODUCTION

The inverter is a device which produces a force proportional to the relative acceleration between its terminals.<sup>1</sup> This can be achieved through various means, including flywheels, rack and pinions or fluid. Inverters have been proposed for automotive and train suspension systems, as well as for vibration control of civil structures during earthquakes.

Semi-active vibration control systems are desirable due to their ability to offer better performance over a wider range of conditions. The benefits of using inverters alongside semi-active dampers in vehicle suspension have been shown.<sup>2</sup> Designs exist for controllable flywheel inverters which use gearboxes<sup>3</sup> or hydraulic valves<sup>4</sup> to adjust the inertance; the use of combined semi-active inverter and damping systems has also been investigated.<sup>5</sup>

To the authors' knowledge, the creation of a semi-active damping device based on the helical inverter<sup>6</sup> has not yet been investigated. Helical inverters work by forcing fluid through a helical tube, creating both an inertial and a damping force. By using magnetorheological (MR) fluid and replacing a small section of the channel with a magnetic valve, it is possible to make the damping force controllable, resulting in a semi-active device.

This paper investigates the feasibility of a helical inverter using MR fluid to achieve semi-active damping. Section 2 discusses the underlying theory for helical inverters and MR valves separately. In Section 3, a dynamic model is created and the effects of adjusting the physical parameters of the device are considered. Section 4 investigates one specific use of the device, as a parallel-layout viscous inverter damper. The paper is concluded in Section 5.

---

Further author information: (Send correspondence to Matthew Tipuric)  
M. Tipuric: E-mail: mrtipuric1@sheffield.ac.uk

## 2. THEORY AND DESIGN

### 2.1 Helical Inerters

Gartner and Smith patented<sup>6</sup> the helical inverter in 2011. Their designs include varieties with either an internal or external helix, as shown in Figure 1. Only the variety with an external helix will be considered here, as this design allows for the addition of an MR valve. The two terminals of the inverter are the cylinder body and the piston rod and the inertance is caused by the mass of fluid in the helix. Viscous effects resist the flow in the helix and largely account for the parasitic damping, with the contributions from the fluid entering and exiting the helix being negligible.<sup>1</sup>

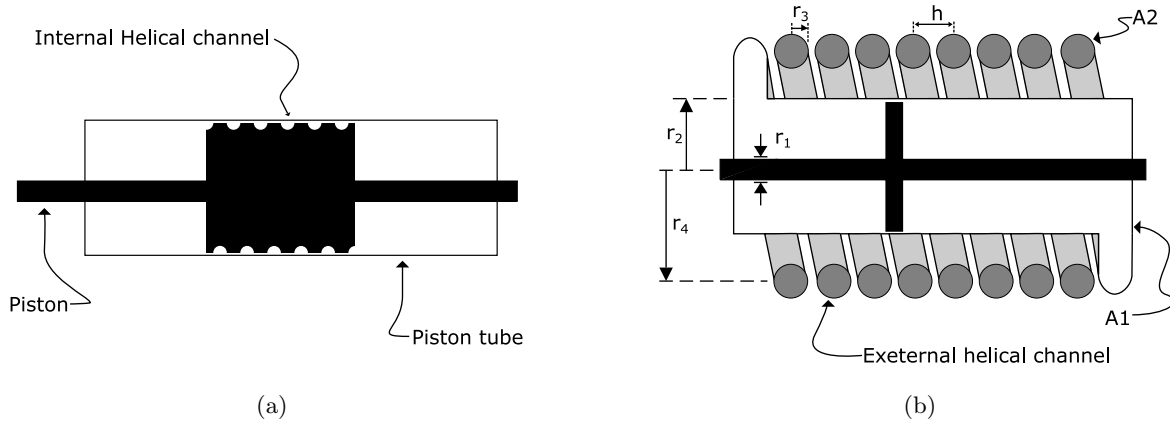


Figure 1: Diagrams of (a) the internal helix design and (b) the external helix design.

The inertance,  $b$ , is measured in kg and creates a force proportional to the relative acceleration of the inverter's terminals. The parasitic damping consists of a linear component,  $c_l$  and a quadratic term,  $c_q$ , which create forces proportional to the relative velocity of the terminals and its square, respectively. Thus the force response helical inverter to a relative displacement across its terminals,  $z$ , is:

$$F = b\ddot{z} + c_l\dot{z} + c_q\dot{z}^2, \quad (1)$$

where

$$\begin{aligned} b &= \frac{m_{hel}}{1 + \frac{h}{2\pi r_4}} \left(\frac{A_1}{A_2}\right)^2, \\ c_l &= 8.77\mu l \pi \left(\frac{A_1}{A_2}\right), \\ c_q &= 0.04845 \frac{\rho l A_1}{\sqrt{r_3 r_4}} \left(\frac{A_1}{A_2}\right)^2 \end{aligned} \quad (2)$$

and  $m_{hel} = \rho n \pi r_3^2 \sqrt{h^2 + (2\pi r_4^2)}$  refers to the mass of the fluid in the helix,  $\mu$  is the viscosity of the fluid,  $\rho$  is the density of the fluid,  $n$  is the number of turns in the helix,  $l$  is the length of the helix and the other parameters are as defined in Figure 1b.

One current use for inerters is passive vibration isolation in civil engineering structures. This is achieved in a similar manner to with a tuned mass damper, converting the peak in the system's transfer function at resonance to two peaks, away from the original natural frequency and with a smaller amplitude, as shown in Figure 2a. As the helical inverter can be modeled as an ideal inverter in parallel with a viscous damper,<sup>1</sup> it lends itself to use in a design known as a parallel-layout viscous inverter damper (PVID),<sup>7</sup> as seen in 2b.

A PVID can be optimised to minimise the maximum magnitude of the response at any frequency ratio using fixed point theory.<sup>8</sup> For any given ratio of the inertance to the structure's original mass,  $\iota = \frac{b}{m}$ , there exist two relevant 'fixed-points', values of the frequency ratio,  $q = \frac{\omega}{\omega_n}$ , for which the transmissibility,  $|\frac{X}{R}|$ , is independent

of damping. The optimum stiffness ratio,  $\lambda = \frac{k}{k_d}$ , is calculated to make the transmissibility equal at both these points and the optimum damping ratio,  $\zeta_{opt}$ , is the root mean square of these values. The method used is only valid for  $\nu \leq 0.5$ , due to discontinuities in the equations involved.

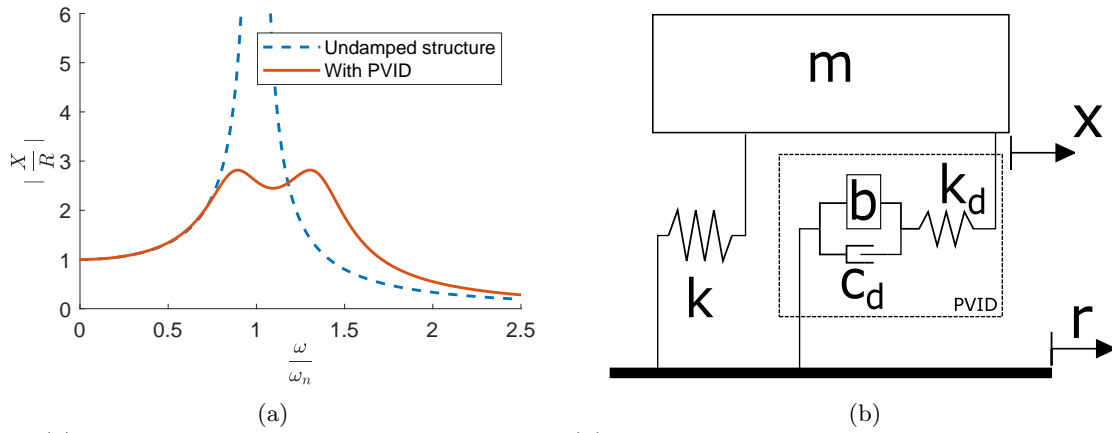


Figure 2: (a) Ideal transfer function of a structure and (b) Dynamic model of a simple structure with a PVID.

## 2.2 Magnetorheological valves

Magnetorheological (MR) fluids are a class of smart material, consisting of magnetisable particles suspended in a non-magnetisable liquid. Exposing the fluid to a magnetic field causes the particles to align, increasing the yield stress of the fluid and thus creating a resistance to flow.<sup>9</sup> MR fluids can be modeled as a Bingham fluid, a type of fluid defined by its relationship of shear stress  $\tau$  to strain rate  $\frac{du}{dy}$ :

$$\tau(y) = \tau_b \text{sgn}(u) + \mu \frac{du}{dy} \quad (3)$$

as seen in Figure 3a.  $\tau_b$  refers to the fluid's Bingham, or yield, stress and  $\mu$  is the fluid's viscosity.

In this paper, only valves with an outer radius equal to that of the the helix will be considered. This limits the potential force the valve can create but simplifies the analysis, as the effects of pressure losses due to fluid expansion and contraction at the valve can be ignored. So, in the case of a Bingham fluid flowing through an annulus of radius  $r_3$ , the pressure drop calculations can be simplified by approximating the geometry to two parallel plates with width  $w = 2\pi r_3$ , provided the annulus gap is sufficiently small compared to the radius. The velocity profile is as shown in Figure 3b and will have the general form

$$u_v(y) = \frac{\Delta P}{2\mu L} y^2 + N_1 y + N_2, \quad (4)$$

where  $N_1$  and  $N_2$  are arbitrary constants.

Using the boundary conditions from Table 1, the overall velocity profile can be found to be<sup>10</sup>

$$u_v(y) = \begin{cases} \frac{\Delta P}{2\mu L} (y^2 - 2y_{PI}y) & \text{for region 1} \\ \frac{\Delta P}{2\mu L} (-y_{PI}^2) & \text{for region 2} \\ \frac{\Delta P}{2\mu L} (y^2 - H^2 + 2y_{PO}(H - y)) & \text{for region 3} \end{cases} \quad (5)$$

The shear stress in the plug is found by differentiating Equation (4),

$$\tau(y) = \frac{\Delta P}{L} y + A \quad (6)$$

so

$$-\tau_b = \frac{\Delta P}{L} y_{PI} + N_1 \text{ and } \tau_b = \frac{\Delta P}{L} y_{PO} N_1 \quad (7)$$

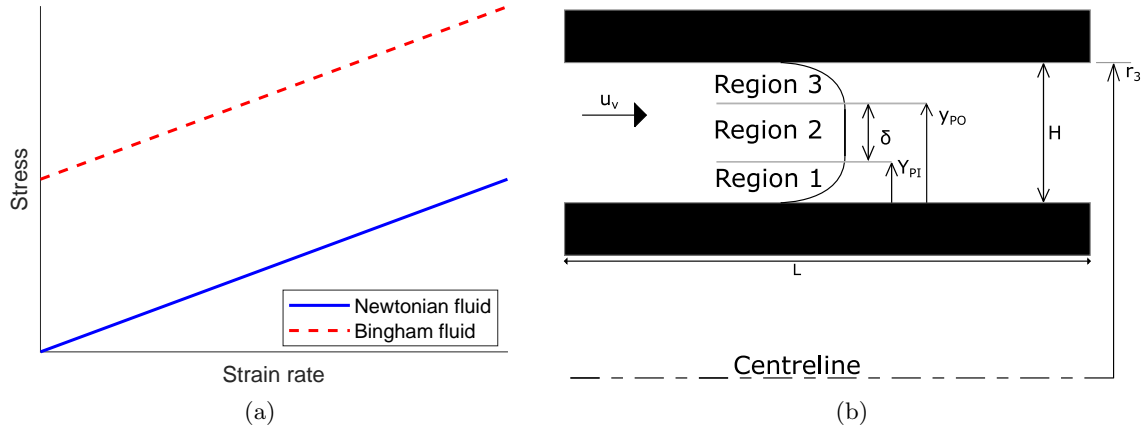


Figure 3: (a) Shear stress/strain rate response of a Bingham fluid and (b) Velocity profile of a Bingham fluid between two parallel plates.

Table 1: Boundary conditions for the three plug regions.

Region 1	$u_v(0) = 0$ $\dot{u}_v(y_{PI}) = 0$
Region 2	$\tau(y_{PI}) = \tau_b$ $\tau(y_{PO}) = -\tau_b$
Region 3	$u_v(H) = 0$ $\dot{u}_v(y_{PO}) = 0$

From this, the plug thickness,

$$\delta = y_{PO} - y_{PI} = \frac{2\tau_b L}{\Delta P}, \quad (8)$$

can be found. By considering geometry, it can be seen that the annulus height  $H = y_{PI} + y_{PO}$ . This leads to

$$y_{PI} = \frac{H - \delta}{2} \text{ and } y_{PO} = \frac{H + \delta}{2} \quad (9)$$

which, when the non-dimensional plug thickness

$$\bar{\delta} = \frac{\delta}{H} \quad (10)$$

is used, becomes

$$y_{PI} = \frac{H(1 - \bar{\delta})}{2} \text{ and } y_{PO} = \frac{H(1 + \bar{\delta})}{2}. \quad (11)$$

When Equations (8) and (10) are combined, the non-dimensional plug thickness becomes

$$\bar{\delta} = \frac{2\tau_b L}{\Delta P H} = \pi_*^{-1}, \quad (12)$$

where  $\pi_*$  is the ratio of wall stress to Bingham stress used in Ref. 11.

When Equations (10) and (12) are substituted into Equation (5), the velocity profile becomes

$$u_v(y) = \begin{cases} \frac{\Delta P}{2\mu L} (y^2 - H(1 - \bar{\delta})y) & \text{for region 1,} \\ \frac{\Delta P}{8\mu L} (H(1 - \bar{\delta}))^2 & \text{for region 2 and} \\ \frac{\Delta P}{2\mu L} (y^2 - (H(1 + \bar{\delta})y + H^2\bar{\delta})) & \text{for region 3.} \end{cases} \quad (13)$$

The flow rate can be found by integration.

$$Q = \begin{cases} -\frac{wd^3\Delta P}{24\mu L}(1-\bar{\delta})^3 & \text{for regions 1 \& 3 and} \\ -\frac{wd^3\Delta P}{8\mu L}(1-\bar{\delta})\bar{\delta} & \text{for region 2.} \end{cases} \quad (14)$$

When these contributions are summed, the total flow rate is found to be

$$Q = -\frac{wd^3\Delta P}{12\mu L}(1-\bar{\delta})^2\left(1+\frac{\bar{\delta}}{2}\right). \quad (15)$$

Using Equation (12) and multiplying by the channel cross sectional area  $A = wH$ , the resistive force created by an MR valve of radius  $r_3$  is found to be

$$F = -\frac{12\mu LwH}{H^2\left(1-\frac{3}{2\pi_*}+\frac{1}{2\pi_*^3}\right)}u_v. \quad (16)$$

As  $\pi_* = \frac{\Delta P h}{2L\tau_b}$ , Equation (16) is dependent on  $\Delta P$ . This dependency can be solved by using a root finding method, as in Ref. 11. Here the flow is non-dimensionalised by using three groups: the friction factor, Reynolds number and the Hedstöm number, defined as  $\pi_1 = \frac{\Delta P H}{2L\rho\bar{u}_v^2}$ ,  $\pi_2 = \frac{\rho\bar{u}_v H}{\mu}$  and  $\pi_3 = \frac{\tau_b\rho H^2}{\mu^2}$ , respectively, and  $\rho$  is the fluid density,  $\mu$  is the viscosity and  $\bar{u}_v$  is the average velocity in the valve. It should be noted that  $\pi_* = \frac{\pi_1\pi_2^2}{\pi_3}$ . It is shown that

$$\pi_1^3 - \left(\frac{3}{2} + 6\frac{\pi_2}{\pi_3}\right)\left(\frac{\pi_3}{\pi_2}\right)\pi_1^2 + \frac{1}{2}\left(\frac{\pi_3}{\pi_2}\right) = 0. \quad (17)$$

This Equation has three roots, of which only the largest returns a meaningful solution.

### 3. PROPOSED DESIGN

A sketch of the device can be seen in 4a. It consists of a piston with a helical channel. Piston motion causes the fluid to flow through the helix, causing the inertance and parasitic damping. A section of the helix has been replaced with an MR valve, which can create an additional damping force. The length of the valve is much smaller than that of the helix, so any effect on the inertance and passive inerter damping terms should be negligible. The working fluid of the device will be an MR fluid, which is denser than either oil or water and so, by considering Equation (2), it can be seen that there will be a corresponding increase in both  $b$  and  $c_{quad}$ . The addition of the valve will also cause an additional pressure loss term caused by the flow constriction, even when the device is in its off state.

By considering basic fluid mechanics,<sup>12</sup> the total pressure drop will also be a linear sum of the constituent pressure drops. This means that the total damping force created is a linear sum of the three damping forces. The device can be modeled as a parallel arrangement of an inerter, a passive (parasitic) damper and a variable damper, as shown in Figure 4b. The equation of motion for the device when subject to free vibration is:

$$b\ddot{z} + c_p\dot{z} + c_q\dot{z}^2 + F_v = 0, \quad (18)$$

where  $c_p = c_l + c_v^{off}$  is a linear parasitic term consisting of the linear part of the inerter damping force and the force created from the flow constriction in the valve in its off-state. Meanwhile  $F_v$  is the active part of the valve damping force, and  $c_l$  can be found from the device parameters using Equation (2)). Finally  $F_v$  and  $c_v^{off}$  require a root finding method, as described in Section 2.2.

The MR valve and fluid in this paper are based on those used in Ref. 13, with dimensions and properties as detailed in Table 2, unless otherwise stated.

Table 2: Parameters of the MR device used in models in this paper.

Channel height (mm)	Length (mm)	$\rho$ ( $kgm^{-3}$ )	$\mu$ ( $Pa\cdot s$ )
0.59	14	3290	0.1

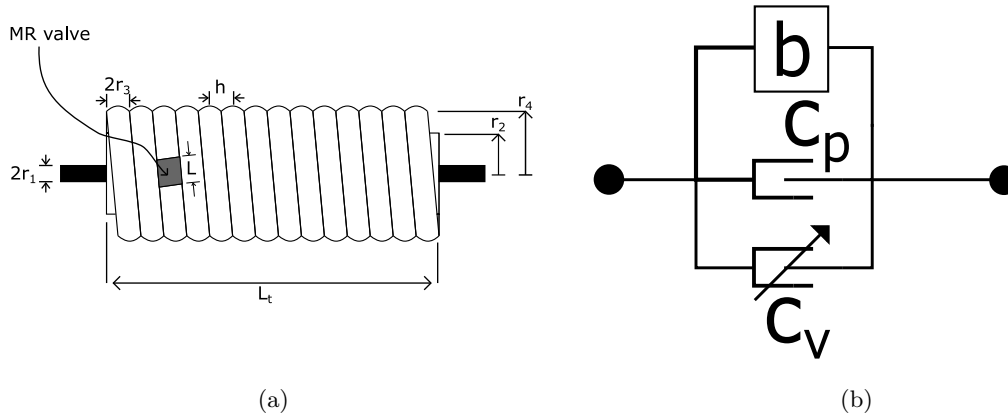


Figure 4: (a) Diagram of the combined device and (b) Dynamic model of the device.

### 3.1 Model

A quasi-static model of the device was created in Matlab. The inputs to the model are the radii of the piston, piston body and the helix, the curve and pitch of the helix, the piston tube length, the length and channel height of the MR valve, the density, viscosity and maximum yield stress of the fluid and the maximum piston velocity. The inertance and damping force contributions by the inerter across the velocity range are found using Equations (1) and (2).

The velocity of the fluid in the valve is calculated using continuity of volume, which allows the Reynolds number  $\pi_2$  to be calculated. The Hedström number is then calculated for the maximum yield stress and for a near zero value (using zero leads to a discontinuity in the equations). The roots of Equation (17) can then be calculated using Matlab’s “roots” function, of which only the largest is meaningful, leaving one value for the friction factor,  $\pi_1$ . This allows the calculation of the pressure drop across the valve at zero and maximum yield stress and thus the damping force created. These are summed with the damping terms from the inerter to produce a force-velocity graph for the inerter, showing the range of allowable damping forces between the minimum and maximum values, of the kind shown in Figure 5a.

### 3.2 Effects of varying parameters

The damping force created by this device is non-linear and dependent on the piston velocity. With a suitable control scheme, it would be possible to select for a given velocity any damping force bounded by the solid lines in Figure 5a; this might be useful for certain control strategies, i.e. Ref. 14. However, to more easily compare with passive devices, it is useful in this instance to linearise the force and use the linear damping coefficients. The best minimum and maximum damping coefficients are defined as those which give the minimum and maximum possible force, respectively, without exceeding the bounds set by the non-linear force-velocity curves, as shown with dashed lines in Figure 5a. It should be noted that that these damping coefficients are dependent on the maximum velocity considered. The ratio of damping coefficients will be referred to as the ‘controllability’ of the device,  $\gamma = \frac{c_{max}}{c_{min}}$ .

From Equation (2), it can be seen that the minimum damping ratio scales with  $\frac{A_1}{A_2} = \frac{r_2^2}{r_3^2}$ , while the valve damping force will scale with the perimeter of the valve  $w = 2\pi r_3$ . Hence, controllability can be improved either by increasing  $r_3$  or decreasing  $r_2$ . This can be seen in Figure 5b, which shows the effects of varying  $r_2$  and  $r_3$  for an inerter with the parameters given in Table 3. However, there is a trade-off with inertance, which scales with  $\frac{r_2^2}{r_3}$ , as shown by Figure 6a.

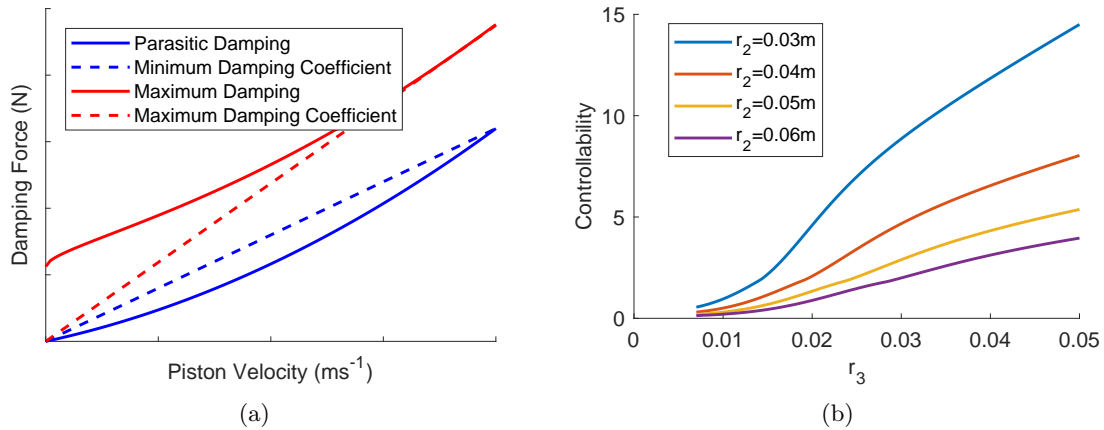


Figure 5: (a) Force-velocity plot and damping coefficients for an arbitrary geometry and (b) Dependence of controllability on  $r_2$  and  $r_3$ .

Table 3: Parameters of the example device (mm unless otherwise stated) used in Figure 5b.

$h$	$r_1$	$r_4$	$L_t$	$\dot{z}_{max}$ (ms <sup>-1</sup> )
100	14	130	600	0.4

Although controllability depends on the ratio  $\frac{A_1}{A_2}$ , it is evident from Equation (2) that this dependency is non-linear. Also, due to the  $m_{hel}$  term in Equation (2), the inertance increases with  $\frac{A_1^2}{A_2}$  and so the relationship between inertance and controllability cannot be easily generalised, even if the ratio is kept the same. For this reason, when designing it is necessary to consider the actual dimensions involved when designing the device, rather than ratio. As an example, Figure 6b considers a range of otherwise identical, unrealistically large, devices, with a constant ratio of areas but increasing absolute values for the radii, as detailed by Table 4. It can be seen that controllability rises non-linearly and asymptotically to 1 with increasing radii. However, it should be noted that increasing the radii in this way increases the mass of the device quicker than the inertance. This causes it to act less like an ideal inerter and might necessitate the inclusion of a parasitic mass in the model.

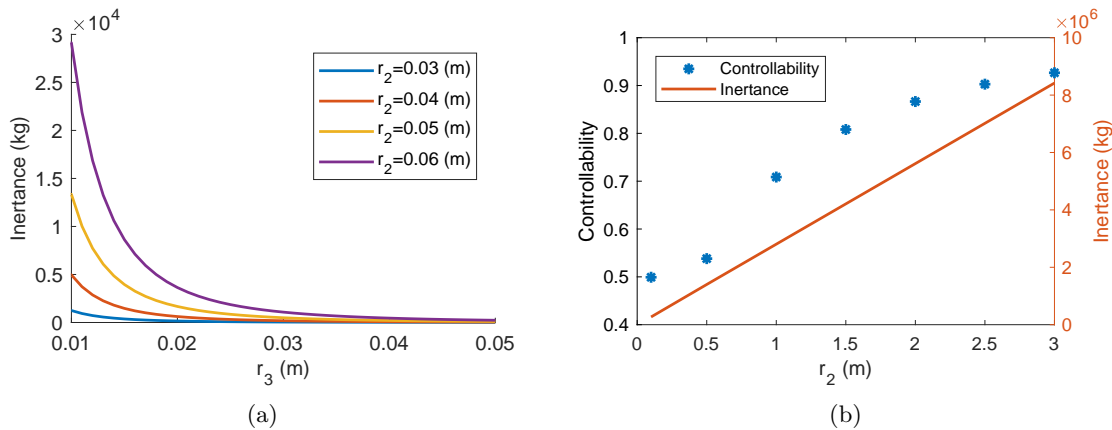


Figure 6: (a) Dependence of inertance on  $r_2$  and  $r_3$  and (b) Dependence of controllability and inertance on piston area at a constant ratio of areas.

Other adjustable parameters are the helix radius,  $r_4$ , the piston tube length,  $L_t$ , the helix pitch,  $h$  and the valve length,  $L$ . The effects of varying these for a device which otherwise has the parameters given in Table 5 can be seen in Figure 7. Changing  $r_4$  or  $L_t$  effectively changes the helix length and so increasing either increases inertance at the expense of controllability. Various bounds exist on these parameters; i.e. in the standard configuration  $r_4$  cannot be smaller than  $r_2 + r_3$ . In addition, increasing either  $r_4$  or  $L_t$  will reduce the compactness of the device. Increasing  $L_t$  will also increase the device's mass. Increasing  $h$  has no desirable effect,

Table 4: Parameters of the inerters compared in Figure 6a.

$h$	$r_1$	$r_2$	$r_3$	$\frac{r_2}{r_3}$	$r_4$	$L_t$	$\dot{z}_{max}$ ( $ms^{-1}$ )
1800	14	100	30	3.33	3900	600	0.4
1800	14	500	150	3.33	3900	600	0.4
1800	14	1000	300	3.33	3900	600	0.4
1800	14	1500	450	3.33	3900	600	0.4
1800	14	2000	600	3.33	3900	600	0.4
1800	14	2500	750	3.33	3900	600	0.4
1800	14	3000	300	3.33	3900	600	0.4

only decreasing inertance, so this parameter should be set as high as possible,  $h = 2r_3$ , to maximise inertance. As it has a negligible effect on the device inertance, in this model, increasing the valve length only improves the controllability of the device, without affecting inertance. However, the magnitude of this increase is small in comparison to varying either  $r_2$ ,  $r_3$  or  $r_4$ . In addition, replacing too much of the helix length with MR valves will decrease the accuracy of the model used in this paper, which assumes that  $l \gg L$ .

Table 5: Default parameters for the device considered in Figure 7 (mm unless otherwise stated)

$h$	$r_1$	$r_2$	$r_3$	$r_4$	$L_t$	$\dot{z}_{max}$ ( $ms^{-1}$ )
30	14	50	15	65	600	0.4

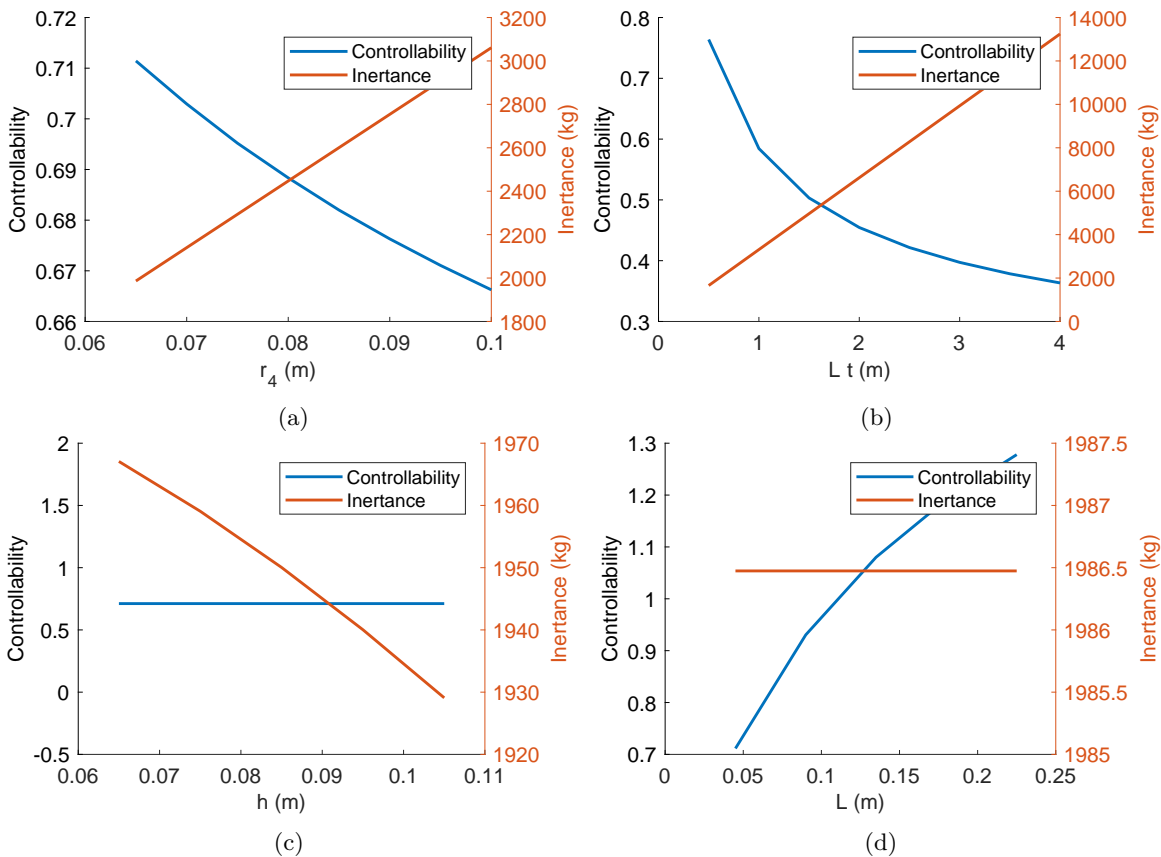


Figure 7: Effects on controllability and inertance of varying (a)  $r_4$ , (b)  $L_t$ , (c)  $h$  and (d)  $L$ .

Table 6: Dimensions of the original inerter (mm).

$r_1$	$r_2$	$r_3$	$r_4$	$H$	$L_t$
14	50	20	130	40	600

Table 7: Original and updated system parameters.

	Original	Updated
$\rho$ ( $kgm^{-3}$ )	999	3290
$\mu$ ( $Pas$ )	0.001	0.1
$\nu$	0.05	0.2
$\zeta_{opt}$	0.07	0.07
$b$ ( $kg$ )	500	1679
Optimum damping ( $kg s^{-1}$ )	890	5922.1
$m$ ( $kg$ )	10,000	8395
$k$ ( $kNm^{-1}$ )	82.2	213.45

#### 4. CASE STUDY

In Ref. 15 a PVID was designed to minimise the transfer function to a structure caused by ground movement. This was achieved by adjusting the parameters of the inerter to create a tuned device, with an optimal trade off between the inertance to mass ratio and the damping ratio. The structure is modeled as shown in Figure 4b and the dimensions of the optimised inerter are given in Table 6. The optimised PVID was modeled with earthquake acceleration data and it was shown that there was a reduction in the magnitude of the response.

This design was used as the basis for an investigation into the semi-active system, with the dimensions kept the same. Due to the viscosity and density of the MR fluid being different to the working fluid of the original device, the updated PVID model was no longer optimised for the original structure. The mass of the structure was updated so that the inertance-mass ratio remained set at  $\nu = 0.2$  and the stiffness was set to optimise the semi-active PVID using the method given in.<sup>8</sup> The new inertance and damping ratio were calculated for the system in its off state, with the damping ratio being found by calculating the total damping force over a range of piston velocities up to  $0.4ms^{-1}$ , and then linearised by the method discussed in Section 3.

This process is, in a way, the reversal of the kind of optimisation that could be used in real world applications; instead of changing the device parameters to match a fixed structure, the device geometry has been kept constant and the host structure adapted to account for the density and viscosity of the MR fluid. The reason for this is simplicity; with so many variables a true optimisation scheme would be complex and, for the purpose of showing the potential of the device, unnecessary. The process is summarised in Figure 8a, with line 1 corresponding to the original device and lines 3 and 6 showing the range of the new, semi-active device. The parameters which were updated are detailed in Table 7.

The stiffness of the PVID can be set to tune the damping of the device in its off-state. In this case study, it was set so the PVID would be under-damped when the MR valve is off (i.e. the fluid is not subject to a magnetic field). It can be seen in Figure 8b that, by increasing the magnetic field strength, the damping of the device can be tuned with the optimal damping ratio of  $\zeta_{opt} = 0.07$  achievable. This could be useful for easily retuning a PVID to take account of changes in a structures properties, such as a change in stiffness caused by heat expansion. The semi-active device could react to such a change and maintain optimal damping.

Increasing the damping ratio of the PVID has a different effect on the transfer ratio depending on the ratio of the frequency of excitation to the natural frequency of the structure. When this frequency ratio falls between the fixed points, increasing the damping actually increases the transfer function, while if the frequency ratio falls outside of these values, increasing the damping ratio leads to a small reduction in the transfer function. A control scheme could be designed to take advantage of this by reactively adjusting the damping ratio to reduce the transfer function created by vibrations close to  $\frac{\omega}{\omega_n} = 1$ , without the increase in vibration away from this zone that would be associated with a passive design. The ability of such a control scheme to cope with multi-frequency content remains to be investigated.

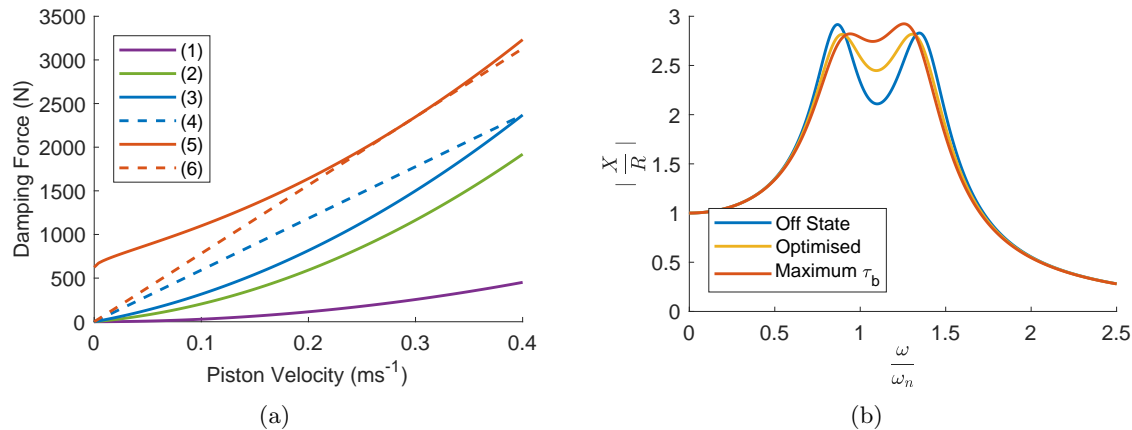


Figure 8: (a) Damping force for the inerter: (1) using oil as the working fluid, (2) using MR fluid, (3) with an MR valve, (4) at the minimum possible damping coefficient, (5) with the MR fluid at maximum Bingham stress, (6) at the maximum damping coefficient and (b) Transfer function against frequency ratio for the PVID.

## 5. CONCLUSION

This paper has looked at a design for a semi-active inerter damper based on a helical inerter design, using magnetorheological fluid. A quasi-static model has been developed and used to investigate the effects of changing the parameters of the device. It has been demonstrated that this model is specific to a given size and range of velocities. It might be necessary to construct a more complex, dynamic modeling the future, to allow for more advanced control schemes.

The quasi-static model was used as part of a case study to demonstrate one potential use for the device as part of a parallel-layout viscous damper. It was shown that the damping force from the magnetorheological valve is large enough to have a meaningful effect on the damping of a large structure and two potential uses for this effect were highlighted. A scheme for optimising the dimensions of the semi-active inerter would maximise this effect, increasing the viability of the design. In addition, the ability of the device to ameliorate multi-frequency signals need to be investigated.

## Acknowledgments

The authors would like to gratefully knowledge the following support. M. Tipuric is supported by EPSRC (grant EP/L016257/1) and P. Deastra is funded by Indonesian Endowment Fund For Education (LPDP).

## REFERENCES

- [1] S. Swift, M. Smith, A. Glover, C. Papageorgiou, B. Gartner, and N. Houghton, "Design and modelling of a fluid inerter," *International Journal of Control* **86**(11), pp. 2035–2051, 2013.
- [2] Z. Xin-Jie, A. Mehdi, and G. Kong-Hui, "On the benefits of semi-active suspensions with inerters," *Shock and Vibration* **19**(3), pp. 257–272, 2012.
- [3] P. Brzeski, T. Kapitaniak, and P. Perlikowski, "Novel type of tuned mass damper with inerter which enables changes of inertance," *Journal of Sound and Vibration* **349**, pp. 56–66, 2015.
- [4] C. Li and M. Liang, "Characterization and modeling of a novel electro-hydraulic variable two-terminal mass device," *Smart Materials and Structures* **21**(2), p. 025004, 2012.
- [5] M. Z. Q. Chen, Y. Hu, C. Li, and G. Chen, "Performance benefits of using inerter in semiactive suspensions," *Control Systems Technology, IEEE Transactions on* **23**(4), pp. 1571–1577, 2015.
- [6] B. J. Gartner and M. C. Smith, "Damping and inertial hydraulic device," (US20130037362 A1), patent filed 2011.
- [7] C. Pan, R. Zhang, H. Luo, C. Li, and H. Shen, "Demand-based optimal design of oscillator with parallel-layout viscous inerter damper," *Structural Control and Health Monitoring* **25**(1), pp. 1–15, 2018.

- [8] Y. Hu, M. Z. Q. Chen, Z. Shu, and L. Huang, "Analysis and optimisation for inerter- based isolators via fixed- point theory and algebraic solution," *Journal of Sound and Vibration* **346**(1), pp. 17–36, 2015.
- [9] J. de Vicente, D. J. Klingenberg, and R. Hidalgo-Alvarez, "Magnetorheological fluids: a review," *Soft Matter* **7**(8), pp. 3701–3710, 2011.
- [10] G. Kamath, "Analysis and testing of bingham plastic behavior in semi-active electrorheological fluid dampers," *Smart Materials and Structures* **5**(5), pp. 576–590, 1996.
- [11] R. Stanway, J. Sproston, and A. Elwahed, "Applications of electro- rheological fluids in vibration control: a survey," *Smart Materials and Structures* **5**(4), pp. 464–482, 1996.
- [12] F. M. White, *Fluid mechanics*, New York, NY : McGraw-Hill Education, 2016, 8th ed., 2016.
- [13] D. Batterbee, "Magnetorheological shock absorbers : modelling, design, and control," *University of Sheffield* , 2006. (Doctoral dissertation).
- [14] M. Ergolu, "Observer based control of an magnetorheological damper," *University of Sheffield* , 2013. (Doctoral dissertation), retrived from <http://etheses.whiterose.ac.uk> (Identification number uk.bl.ethos.581682).
- [15] P. Deastra, D. J. Wagg, and N. D. Sims, "The realisation of an inerter-based system using fluid inerter," *To appear in Proceedings of the 36th IMAC* , 2018.